Formation of Double Layers and Electron Holes in a Current-Driven Space Plasma

D. L. Newman,[1,*] M. V. Goldman,[1] R. E. Ergun,[2] and A. Mangeney[3]

[1]*Center for Integrated Plasma Studies, University of Colorado at Boulder, Boulder, Colorado 80309*

[2]*Laboratory for Atmospheric and Space Physics, University of Colorado at Boulder, Boulder, Colorado 80309*

[3]*DESPA, Observatoire de Meudon, Meudon, France*

(Received 14 September 2001; published 28 November 2001)

Kinetic 1D simulations reveal that a weak density depression in a current-carrying plasma can lead to the formation of a strong potential ramp (double layer). The ramp and plasma turbulence it creates share many features with recent particle and field measurements in the auroral ionosphere. An electron beam accelerated by the ramp produces a series of propagating electron phase-space holes via a spatial two-stream instability. Electron heating associated with the formation and merging of these holes is found to influence the subsequent evolution of the potential ramp.

DOI: 10.1103/PhysRevLett.87.255001 PACS numbers: 52.35.Mw, 52.65.Ff, 94.20.Rr, 94.20.Ss

It has long been recognized that a class of electrostatic structures generally referred to as double layers (DLs) can support a potential jump confined to a narrow spatial region in a current-carrying collisionless plasma [1,2]. This potential "ramp" is associated with a localized parallel electric field (i.e., $\mathbf{E} \parallel \mathbf{B}$, where $\mathbf{B}$ is a background magnetic field). DLs have been observed in laboratory experiments [3–6] as well as in space [7–11], and have been the subject of numerical simulations [12–16] and theoretical studies [17–19].

The importance of DLs in the near-Earth space environment has been made clear by the recent measurement of a well-resolved strong localized dc parallel electric field by the FAST (Fast Auroral SnapshoT) satellite in the downward current region of the auroral ionosphere [10]. These observations reveal the parallel electric field peaking at 250 mV/m and localized to ~100 m along $\mathbf{B}$. The relative motion between the structure and the satellite implies a potential jump of ~25 V, which is capable of strongly accelerating the $\lesssim$2 eV "cold" electron population on the low-potential side. Additional observations indicate the presence of intense very-low-frequency turbulence on the high-potential side of the dc field structure — interpreted as a signature of electron phase-space holes. (Waveform data were not available for this event.) The development of electron holes is consistent with the nonlinear evolution of a two-stream instability [20] driven by electrons accelerated through the ramp. An intriguing feature of the measured fields is the existence of a spatial "gap" between the dc field and the VLF turbulence. A second event with similar characteristics but with an even larger (~750 mV/m) peak dc field has since been analyzed [11]. For both events, $\Delta\phi/T_e \sim 10$, where T_e is the temperature of the cold electron population on the low-potential side.

In this Letter, we will present the results of new kinetic simulations designed to study the development and evolution of a DL and associated turbulence in an initially field-free current-carrying plasma. We will show that the electric fields that develop are in qualitative and often quantitative agreement with the recent FAST observations. To put the present work in the context of past numerical and analytical studies, we first address a fundamental question regarding the formation of DLs in the auroral ionosphere: Is the primary driver a potential drop or a current? The magnetosphere-ionosphere current system at auroral latitudes involves processes on a spatial scale immense compared to the tens of Debye lengths of the observed dc field structure. In laboratory plasmas, DLs are usually created by externally imposing a potential difference along $\mathbf{B}$. In the auroral region under consideration here, it is more likely that the plasma initially carries a current due to larger-scale processes, and that this current drives the formation of a DL at the site of some inhomogeneity, with the resulting potential jump being an *effect* rather than a *cause* of the DL.

Carlqvist [18] speculated theoretically that a DL could develop in a current-driven plasma at the site of a density depression. Early current-driven particle simulations [12] confirmed that a minimum current — subject to the Bohm condition [2] — is necessary to form a DL. Other early DL simulations were driven by an imposed potential drop across the simulation domain [14], or employed a periodic potential [15]. Recent simulations [16] have shown that a potential-driven DL can result in the quasicontinuous generation of electron phase-space holes having electric field signatures consistent with satellite observations.

The new simulations described here address the development of a current-driven DL in the presence of an initial density perturbation, which deepens significantly as the DL grows. These simulations employ a 1D open boundary Vlasov code based on the time-advance algorithm of Cheng and Knorr [21]. We note that a 1D treatment precludes interactions involving oblique wave modes such as electrostatic whistlers, lower-hybrid waves, and ion cyclotron modes, which have been found to play a role in 2D periodic simulations of the electron two-stream instability in the auroral ionosphere [20,22].

The phase-space domain is distributed on a $N_x = 256 \times N_v = 128$ grid that spans the region $0 \le x \le L_x = 640\lambda_e$ and $-15v_\alpha \le v \le 15v_\alpha$ where λ_e is the

initial electron Debye length and $v_\alpha = (T_\alpha/m_\alpha)^{1/2}$ is the *initial* thermal velocity of species $\alpha = e, i$. An ion to electron mass ratio of $M_i/m_e = 400$ is used. We choose as our base distributions counterstreaming electrons and ions that are both Maxwellians drifting, respectively, to the right and left at velocities $u_e = v_e$ and $u_i = -v_i$, with $T_e = T_i$. Thus, the initial electron and ion drifts satisfy both the Bohm and Langmuir conditions [2]. These initial distributions were chosen so that the DL would remain approximately stationary in the frame of the simulation. They are marginally stable to the Buneman instability, which does not preclude the later development of Buneman-like instabilities in the evolved distributions.

We model an unbounded segment of the ionospheric plasma by allowing the potentials at the ends of the simulation domain to float. Without loss of generality, we set $\phi = 0$ at $x = 0$. We also set $E_x = 0$ at $x = 0$, which assumes that the left boundary is not strongly influenced by the evolution of the plasma in the interior of the simulation (we terminate the simulation when this condition ceases to hold). For $x > 0$, the field E_x and the potential ϕ are evaluated via the first two integrals of the charge density. Total charge neutrality in the simulation domain is not imposed, but electric fields at the right boundary that develop as a result of any net charge imbalance act self-consistently to restore neutrality.

We impose an inhomogeneity in the initial state in order to "seed" the formation of a DL. This charge-neutral perturbation takes the form $n_\alpha(x)/n_0 = 1 - a\cos^2[(x - x_0)/w]$ with $a = 0.125$, $x_0 = L_x/2$, and $w = 160\lambda_e$. The initial currents J_e and J_i are both made spatially uniform by adjusting the mean velocity u_α so that the particle flux $n_\alpha v_\alpha$ is constant. The initial 12.5% depression is shallow relative to the ~80% depression that eventually develops in the simulation. A comparison run with the initial density depression reduced by a factor of 2 shows all of the phases of DL evolution discussed below, following an initial delay of $\sim 2500\omega_e^{-1}$. Thus, the depth of the initial perturbation does not appear to be a critical parameter in our simulations.

The key features of the evolution of the plasma can be seen in the electron (Fig. 1) and ion (Fig. 2) phase-space distributions (see Ref. [23]). Figure 3 contains time histories of the electrostatic potential ϕ and ion density n_i in the region $40\lambda_e \le x \le 600\lambda_e$.

There is little visible development in the interval $0 < \omega_e t \lesssim 500$, during which the evolution follows the path suggested by Carlqvist [18]. After $\omega_e t = 500$, the $x \gtrsim 350\lambda_e$ region of Fig. 3a is dominated by a series of unipolar potential pulses moving toward the right boundary. A "snapshot" of electron phase-space density f_e at $\omega_e t = 1000$ (Fig. 1a) clearly shows the electron holes that are associated with the potential pulses. Ion phase space (Fig. 2a) shows only weak perturbations at this time. Neither f_e nor ϕ show any clear evidence of a DL at this point.

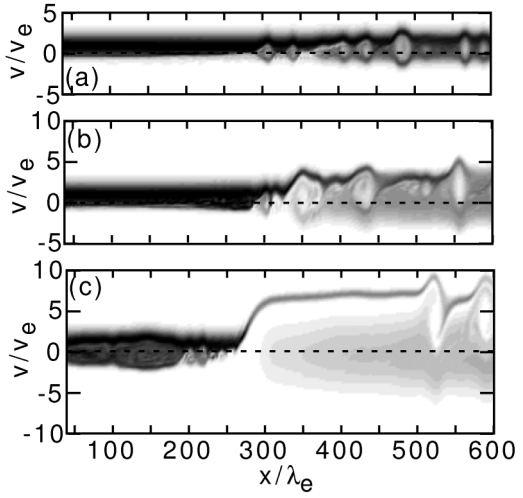

FIG. 1. Contour maps of $f_e(x, v)$ at three fixed times: (a) $\omega_e t = 1000$; (b) $\omega_e t = 2500$; (c) $\omega_e t = 4000$.

After $\omega_e t \approx 2000$, the situation changes. Figures 1b and 2b show f_e and f_i at $\omega_e t = 2500$. The electron holes are significantly larger than at $\omega_e t = 1000$, and are embedded in a hotter electron distribution. The need to properly account for the heating of electrons on the high-potential side of the ramp motivates the following boundary conditions on the particle distributions: f_e at the right boundary ($x = L_x$) is continuously adjusted to equal the distribution averaged over a narrow ($40\lambda_e$) zone near $x = L_x$. The ion distribution is similarly adjusted at $x = 0$. Use of these "adaptive" boundary distributions reflects the fact that the ends of the simulation domain do *not* correspond to physical boundaries in the plasma being modeled. In the ionosphere, the electron holes and their embedding distribution would fill an ever expanding region on the high-potential side of the ramp. Thus, f_e at $x = L_x$ is better represented by f_e in the interior of the simulation than by the *initial* boundary distribution. Comparable phase-space evolution was found in an otherwise identical reference simulation run with N_x and L_x both

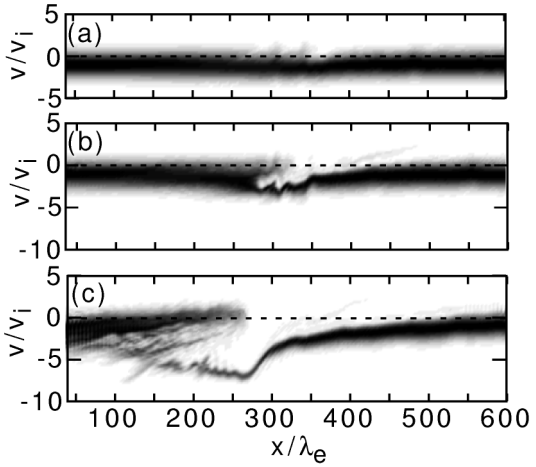

FIG. 2. Contour maps of $f_i(x, v)$ at three fixed times: (a) $\omega_e t = 1000$; (b) $\omega_e t = 2500$; (c) $\omega_e t = 4000$.

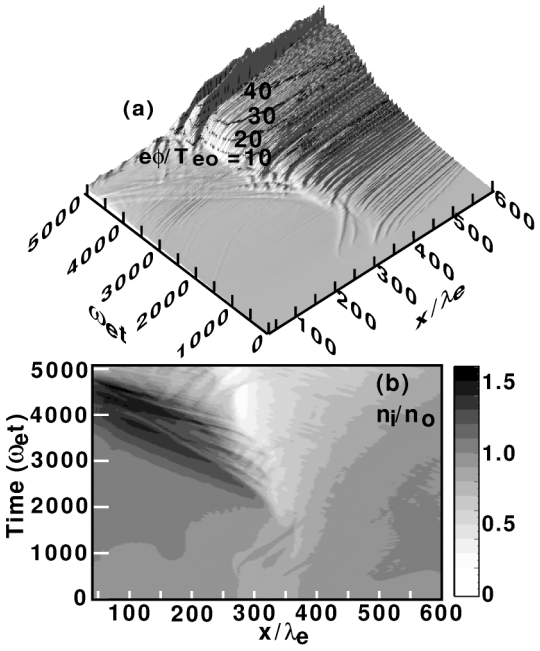

FIG. 3. Time histories of (a) the electrostatic potential $e\phi(x,t)/T_{e0}$ and (b) the ion density n_i/n_0 from the primary simulation run. Contours of $e\phi/T_{e0}$ =10, 20, 30, and 40 are shown as dark bands on the elevated surface plot in frame (a).

increased by a factor of 2, which implies that our results are not significantly biased by the simulation box size or boundary conditions.

An accelerated electron beam is clearly evident in Fig. 1b at $\omega_e t = 2500$, although the potential (Fig. 3a) still does not exhibit the characteristics of a well-defined ramp. Instead, ϕ is quite irregular near the center of the simulation box. There is also a clearly defined ion beam (Fig. 2b), which shows modulations in velocity indicative of perturbations due to a wave. A linear stability analysis using the evolved electron and ion distributions from related simulations reveal conditions conducive to strong growth due to effective cooling of the ion beam [24]. Potential pulses moving slowly toward the left (small x) starting at $\omega_e t \approx 2500$ in Fig. 3(a) are a signature of these waves, which trap both electrons and ions. The ion density (Fig. 3b) also shows large perturbations, with a maximum 50% density depression at $x = 320\lambda_e$ and a 25% overdensity at $x = 250\lambda_e$. This density enhancement marks the formation of an ion "front" that propagates to the left at approximately the ion acoustic speed.

Only after time $\omega_e t = 3500$ does a "classical" DL form. The well-defined potential ramp is clearly visible in Fig. 3a, as is the coincident ~80% density depression in Fig. 3b. Electron and ion phase space at $\omega_e t = 4000$ (Figs. 1c and 2c) also show beam acceleration characteristic of a strong unipolar dc electric field. At this point, the potential jump across the steepest section of the ramp has a potential difference $\Delta\phi/T_e \gtrsim 20$, which is in reasonable agreement with the best estimates based on the FAST observations.

Figure 4 contains a comparison of E_x from the simulation (over the time interval $3700 \leq \omega_e t \leq 4400$) with dc and rms fluctuating fields observed by FAST [10]. The simulation field in Fig. 4a, which scales as $(n_e T_e)^{1/2}$, is evaluated for a plasma with $n_e T_e$ = 55.3 eV cm^{-3}—consistent with measured values [10]. The horizontal axis is also scaled, with optimal agreement occurring for $\lambda_e = 5 \pm 2.5$ m in the simulation—somewhat larger than the measured upstream value of 1.5 m [10]. The simulated and observed rms fields in Fig. 4b show similar behavior, with a region of approximately linear slope (indicated by the dashed line segments) on the high-potential side of the strong dc field. This feature suggests a region of linear spatial growth driven by the two-stream instability, and accounts for the observed gap between the dc peak and the VLF turbulence in the observations. The longer growth length in the simulation may be due to differences in the trapped electron population resulting in a larger group velocity, a slower temporal growth rate, or some combination of the two. Despite the differences in growth length and wave level on the low-potential side, both the simulated and observed fields saturate for $E_{\rm rms} \approx 100$ mV/m.

In the simulation, the smooth potential ramp is disrupted at time $\omega_e t \approx 4500$. Phase-space plots (not shown) reveal that this disruption is due to the growth of a large electron hole on the leading (low-potential) edge of the ramp. A preliminary analysis [24] indicates that this hole may be the result of a Buneman-like instability involving the interaction of accelerated electron and ion distributions. When this hole becomes sufficiently large, it begins to accelerate

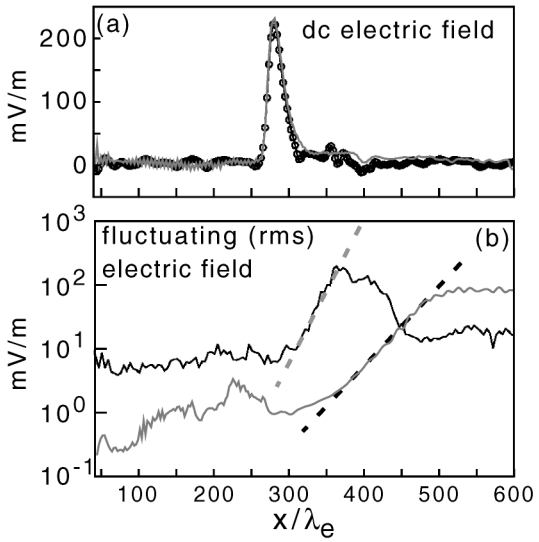

FIG. 4. Simulation electric fields over time interval $3700 < \omega_e t < 4400$ as a function of position. (a) The gray curve is $-E_{\rm dc}$ superimposed on the dc field measured by FAST (black) from Fig. 4a of Ref. [10]. (b) The gray curve is the simulation rms oscillating field. The black curve is the rms field measured by FAST from Fig. 4b of Ref. [10]. The dashed line segments are fits to the inferred linear growth region on each curve.

in the direction of the electron flow, eventually overtaking smaller electron holes formed on the high-potential side of the ramp by the electron two-stream instability.

The FAST measurements [10] imply that the observed DL remains intact for at least $\sim$100 ms $\approx 4 \times 10^4 \omega_e^{-1}$ for $f_e = \omega_e/2\pi \approx 70$ kHz. Although this is significantly longer than the lifetime of the DL in our simulation, the larger (physical) ion mass in the ionosphere is expected to translate into longer time scales for ion-mediated events. Growth rates of the electron-ion instabilities responsible for disrupting the DL can also depend sensitively on details of the initial distribution functions.

The mean electron drift velocity u_e near the right boundary remains nearly constant throughout the simulation run. By contrast, the electron thermal velocity v_e (defined as the rms velocity in the mean drift frame) increases steadily throughout most of the run, leveling off to a value $v_e \approx 4v_{e0}$ during the time interval containing the strong DL ($\omega_e t \approx 4000$). Thus, the ratio of drift to thermal velocity decreases from an initial value $u_e/v_e = 1$ down to $u_e/v_e \approx 0.25$ at $\omega_e t = 4000$. This ratio is expected to decrease with distance from the DL, as the merging of electron holes further heats the plasma. A value smaller than 0.25 would be consistent with FAST measurements [25] of the ratio u_e/v_e during times when the field signatures of electron holes were observed. Specifically, the measured distribution of values peaks for u_e/v_e between 0.1 and 0.2, with a tail of decreasing probability for higher values.

The simulations presented here show that a strong electrostatic DL that shares many features with a recently observed DL in the auroral ionosphere can develop from a weak density perturbation in a current-carrying plasma. The spatial form of the dc electric field agrees very well with the observed dc field. There is also good qualitative agreement between the fluctuating rms fields associated with the formation of electron holes via a two-stream instability. We note that electron holes are created throughout the duration of the simulation, including times well before the formation of a clearly defined DL potential ramp, and that the heating of the electron distribution that occurs in connection with these "early" electron holes appears to be a prerequisite for the formation of a strong DL. These simulations thus suggest that the presence of a strong DL might be *sufficient* but not *necessary* for electron-hole generation.

This research was supported by grants from NSF (ATM-9802209), NASA (NAG5-9026), and DOE (DE-FG03-98ER54502). Computations were performed at NCAR, the Advanced Computing Laboratory at LANL, and at NERSC.

*Email address: David.Newman@colorado.edu

[1] I. Langmuir, Phys. Rev. **33**, 954 (1929).
[2] L. P. Block, Astrophys. Space Sci. **55**, 59 (1977).
[3] P. Coakley and N. Hershkowitz, Phys. Fluids **22**, 1171 (1979).
[4] K. Saeki, P. Michelsen, H. L. Pécseli, and J. J. Rasmussen, Phys. Rev. Lett. **42**, 501 (1979).
[5] P. Leung, A. Y. Wong, and B. H. Quon, Phys. Fluids **23**, 992 (1980).
[6] Y. Takeda and K. Yamagiwa, Phys. Fluids B **3**, 288 (1991).
[7] M. Temerin, K. Cerny, W. Lotko, and F. S. Mozer, Phys. Rev. Lett. **48**, 1175 (1982).
[8] R. Boström, G. Gustafsson, B. Holback, G. Holmgren, H. Koskinen, and P. Kintner, Phys. Rev. Lett. **61**, 82 (1998).
[9] F. S. Mozer and C. A. Kletzing, J. Geophys. Res. **25**, 1629 (1998).
[10] R. E. Ergun, Y.-J. Su, L. Andersson, C. W. Carlson, J. P. McFadden, F. S. Mozer, D. L. Newman, M. V. Goldman, and R. J. Strangeway, Phys. Rev. Lett. **87**, 045003 (2001).
[11] L. Andersson, R. E. Ergun, D. Newman, J. P. McFadden, and C. W. Carlson, Phys. Plasma (to be published).
[12] C. K. Goertz and G. Joyce, Astrophys. Space Sci. **32**, 165 (1975).
[13] G. Joyce and R. F. Hubbard, J. Plasma Phys. **20**, 391 (1978).
[14] N. Singh, Plasma Phys. **24**, 639 (1982).
[15] N. Singh and R. W. Schunk, Plasma Phys. Controlled Fusion **26**, 859 (1984).
[16] N. Singh, Geophys. Res. Lett. **27**, 927 (2000).
[17] L. P. Block, Cosmic Electrodyn. **3**, 349 (1972).
[18] P. Carlqvist, Cosmic Electrodyn. **3**, 377 (1972).
[19] H. Schamel, Phys. Rep. **140**, 161 (1986).
[20] M. V. Goldman, M. M. Oppenheim, and D. L. Newman, Geophys. Res. Lett. **26**, 1821 (1999).
[21] C. Z. Cheng and G. Knorr, J. Comput. Phys. **22**, 330 (1976).
[22] F. J. Crary, M. V. Goldman, R. E. Ergun, and D. L. Newman, Geophys. Res. Lett. **28**, 3059 (2001).
[23] See AIP Document No. EPAPS: E-PRLTAO-87-023151 for video of f_e and f_i over the duration of the run. This document may be retrieved via the EPAPS homepage (http://www.aip.org/pubservs/epaps.html) or from ftp.aip.org in the directory /epaps/. See the EPAPS homepage for more information.
[24] M. V. Goldman, D. L. Newman, R. E. Ergun, and A. Mangeney, Nonlin. Proc. Geophys. (to be published).
[25] R. E. Ergun, C. W. Carlson, L. Muschietti, I. Roth, and J. P. McFadden, Nonlin. Proc. Geophys. **6**, 187 (1999).